

Direct-joining of a polylactide acid-hydroxyapatite biocomposite with a titanium alloy

Renan Aduino¹, Gean Henrique Marcatto de Oliveira¹ , Mário Augusto Morozo¹ , Márcio Antônio Fiori² 
and Leonardo Bresciani Canto^{1,3*} 

¹Programa de Pós-Graduação em Ciência e Engenharia de Materiais – PPGCEM, Universidade Federal de São Carlos – UFSCar, São Carlos, SP, Brasil

²Departamento de Física, Universidade Tecnológica Federal do Paraná, Pato Branco, PR, Brasil

³Departamento de Engenharia de Materiais – DEMa, Universidade Federal de São Carlos – UFSCar, São Carlos, SP, Brasil

*leonardo@ufscar.br

Abstract

A promising yet underexplored alternative for biomedical applications involves incorporating polymer, metal, and ceramic materials into hybrid structures. In this study, a biocomposite consisting of polylactic acid (PLA) with 20 wt% of nearly spherical sub-micron hydroxyapatite (HA) particles was successfully synthesized. The HA particles were uniformly dispersed and distributed within the PLA matrix, leading to a biocomposite with a well-balanced combination of thermal and mechanical properties. This PLA–HA biocomposite was then directly joined through injection overmolding onto a laser-surface-structured titanium alloy Ti6Al4V substrate. The PLA–HA/Ti6Al4V hybrid joints demonstrated robust mechanical anchorage, achieved through the thorough filling of the polymer biocomposite into the micro-scale structures engineered onto the metal surface. This mechanism ensured good lap-shear strength, making these hybrid joints promising candidates for orthopedic applications.

Keywords: *polymer-metal hybrids, polylactide acid, hydroxyapatite, injection overmolding.*

How to cite: Aduino, R., Oliveira, G. H. M., Morozo, M. A., Fiori, M. A., & Canto, L. B. (2025). Direct-joining of a polylactide acid–hydroxyapatite biocomposite with a titanium alloy. *Polímeros: Ciência e Tecnologia*, 35(1), e20250009. <https://doi.org/10.1590/0104-1428.20240095>

1. Introduction

The development of new materials for biomedical applications has advanced significantly. Single-class material structures often fail to meet all the requirements for specific applications. Consequently, combining different material classes has become a common approach to achieve the desired properties.

Biocomposites of polylactic acid (PLA) and hydroxyapatite (HA) have been the focus of intense research aimed at advancing biomaterials and tissue regeneration^[1-8]. Polylactic acid (PLA), an aliphatic thermoplastic polyester from renewable resources, stands as one of the most extensively researched and widely utilized polymers in biomedical applications. Granted approval by the United States Food and Drug Administration (FDA) for medical use, PLA boasts biodegradability, biocompatibility, and ease of processing^[1]. Hydroxyapatite (HA) is a calcium phosphate ($\text{Ca}_{10}(\text{PO}_4)_6(\text{OH})_2$) with composition similar to that of biological apatite found in human hard tissues, making it ideal for orthopedic and dental applications^[9,10]. The incorporation of HA into PLA enhances the resemblance of the biocomposite to natural bone tissue, conferring osteobiological properties suitable for targeted biomedical applications^[1-4]. Increasing HA content in the PLA matrix

improves its degree of crystallinity^[5-7], reduces thermal stability^[6,7], and slows down hydrolytic degradation^[8]. Furthermore, the addition of HA increases the elastic modulus but compromises tensile strength and elongation at break^[6,7].

Meanwhile, titanium alloy Ti6Al4V is distinguished as a widely used metal alloy for bone-anchoring implants, prized for its unique combination of beneficial attributes. These include a comparable elastic modulus to bone, outstanding fatigue resistance, favorable hardness, lightweight construction, remarkable corrosion and wear resistance, minimal ion release rates, biocompatibility, and hypoallergenic nature^[11,12]. Moreover, Ti6Al4V has been modified with HA through composites^[13] and coatings^[14] to satisfy the specific demands of biomedical applications.

The integration of a PLA–HA biocomposite with a Ti6Al4V titanium alloy into a single structure remains an unexplored approach, but one with significant potential to meet a wide range of mechanical, physicochemical and biological requirements for biomedical applications. The use of injection overmolding with direct-adhesion is particularly advantageous for this purpose, as it is a well-established and highly efficient processing method for assembling polymer-metal hybrids of various sizes and

shapes, combining automation, high-speed production, cost-effectiveness, precise dimensional control, and exceptional bond strength^[15,16]. Optimal adhesion between polymer and metal parts in injection overmolding can be further enhanced by preparing the metal surface with laser structuring^[17-19].

This study investigates the direct-joining of a biocomposite consisting of polylactic acid (PLA) and hydroxyapatite (HA) with a Ti6Al4V titanium alloy for biomedical applications, using metal laser structuring and injection overmolding techniques. The research focuses on the preparation of the biocomposite via melt-state processing, as well as its morphological, thermal, and mechanical characterization, alongside the manufacturing process, interfacial characterization, and evaluation of the joining strength of the PLA–HA/Ti6Al4V hybrid.

2. Materials and Methods

2.1 Materials

Poly lactide acid (PLA) is a commercial grade (IngeoTM 4043D) supplied by NatureWorks company with density of 1.24 g/cm³. It has a number-average molecular weight of 41 kg/mol and weight-average molecular weight of 76 kg/mol^[8].

Hydroxyapatite (HA) with a Ca/P molar ratio of 1.71 was synthesized in an aqueous medium through the precipitation method. The precursors used were calcium oxide (CaO, 95%) and phosphoric acid (H₃PO₄, 85%), with ammonium hydroxide (NH₃OH, 30%) acting as the pH regulator. A total of 159.1 g of calcium oxide was added to 1000 mL of distilled water in a 1500 mL beaker. The mixture was stirred for 24 hours at 25°C using a mechanical stirrer set at 1000 rpm, forming a Ca(OH)₂ suspension with excess distilled water. Next, a solution of 194.6 g of 85% phosphoric acid was added to the suspension at a rate of 1.8 mL/min. During the addition, the pH was monitored using universal pH indicator strips. The suspension was then stirred for 4 hours at 80°C. At the end of this period, the pH was adjusted to 7 by adding 37.6 g of ammonium hydroxide. The final suspension was left to rest for 24 hours to stabilize the pH and allow the formation of a liquid phase and precipitate. The precipitate was separated

from the suspension by filtration using Whatman filter paper (No. 1) and a vacuum pump. The filtered material was then dried in an oven at 100°C for 24 hours. After drying, the sample was cooled in a desiccator to room temperature. It was then ground into a fine powder using a mortar and agate pestle. The dried powder was subsequently calcined in a muffle furnace with a heating rate of 8°C/min until it reached 800°C, where it remained for 2 hours. The characterization of hydroxyapatite is shown elsewhere^[20].

Ti6Al4V ELI is a 3.5 mm thick rolled sheet supplied by Shaanxi Aone Titanium Metal Materials Company (China).

2.2 Experimental procedure

The experimental workflow of this study is depicted in Figure 1. It involved two main stages: the preparation and characterization of the PLA–HA biocomposite, and the joining of the PLA–HA biocomposite onto a Ti6Al4V substrate, followed by its mechanical and interfacial characterization.

2.3 Preparation and characterization of the PLA–HA biocomposite

A PLA–HA biocomposite with 20 wt% filler was prepared using the melt-compounding procedure described below. The filler content was selected based on the study conducted by Ferri et al.^[6], which demonstrated that this composition provides a good balance of mechanical properties.

The PLA–HA biocomposite was produced using an APV Baker Perkins Equipment and Systems intermeshing co-rotating twin-screw extruder (model MP-19TC) with a 19 mm screw diameter (D) and a length to diameter ratio (L/D) of 25:1. The barrel temperature was maintained at 200°C, and the screw speed was set to 100 rpm. Before processing, PLA pellets were cryogenically ground into a fine powder using a CF Bantam Micron Powder Systems mill. The dried powders of PLA and HA were mixed thoroughly in the desired ratio and fed into the extruder at a rate of 2.4 kg/h using a Brabender feeder. The extruded strands were cooled in a water bath immediately after exiting the die and then pelletized.

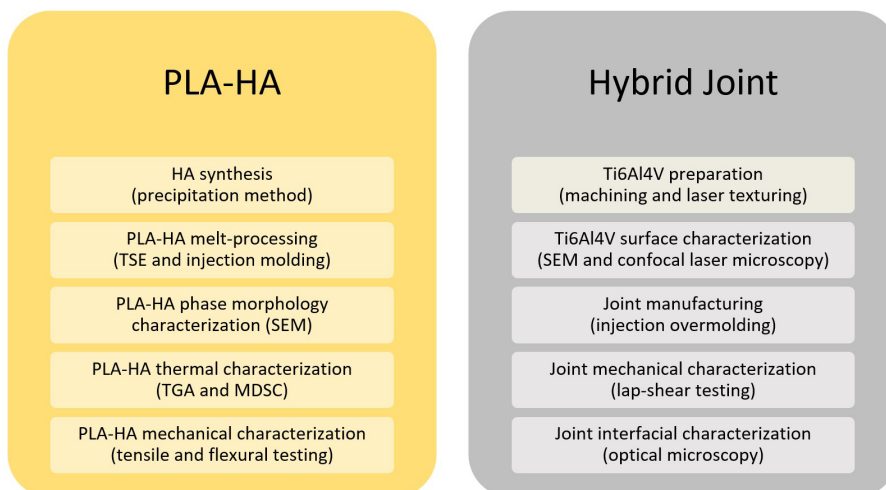


Figure 1. Experimental workflow.

Specimens (Type I tensile bars – ASTM D638) were injection molded using an Arburg Allrounder 270V 300-120 machine with the following parameters: a barrel temperature of 200°C, an injection speed of 50 cm³/s, a holding pressure of 250 bar for 7 seconds, a mold temperature of 25°C, and a cooling time of 55 seconds.

The phase morphology of the PLA–HA biocomposite was examined using scanning electron microscopy (SEM) with an FEI Inspect S50 instrument, operating at an acceleration voltage of 10 kV and a magnification of 20,000. A sample taken from the injection-molded specimen was fractured after being immersed in liquid nitrogen and subsequently sputter-coated with gold before undergoing SEM examination. The morphology of the hydroxyapatite (HA) was evaluated using SEM with an FEI Magellan 400 L instrument, operating at an acceleration voltage of 7 kV and a magnification of 170,000. The HA sample was dispersed in ethyl alcohol using ultrasound, dripped onto a thin aluminum sheet, and then sputter-coated with gold before SEM analysis.

The thermal decomposition of PLA in both neat PLA and PLA–HA samples was assessed using thermogravimetric analysis (TGA) with a TA Instruments Q500. Samples (15 ± 0.5 mg) were taken from the inner section of the injection-molded specimens and heated from 25 to 800°C at a rate of 20°C/min under a nitrogen atmosphere (50 mL/min).

The crystallinity of PLA in both neat PLA and PLA–HA samples was analyzed using modulated differential scanning calorimetry (MDSC) with a TA Instruments DSC Q2000. Samples (11 ± 0.5 mg) were taken from the inner section of the injection-molded specimens and scanned from 25°C to 200°C at a heating rate of 2°C/min, with a modulation period of 60 s and an amplitude of 0.318°C, under a nitrogen atmosphere (50 mL/min), following the procedure outlined in^[21].

Tensile testing was performed according to ASTM D638 on injection-molded Type I specimens using an Instron 5569 system, with a crosshead speed of 5 mm/min. Flexural testing was conducted following ASTM D790 on standard bars machined from injection-molded specimens, using the Instron 5569 system, with a crosshead speed of 1.27 mm/min. Five replicate specimens were tested, which were conditioned at 23°C and 50% relative humidity for 48 hours before testing.

2.4 Joining of PLA–HA biocomposite onto a Ti6Al4V substrate

Hybrid joints with a half-lap splice configuration (Figure 2) were fabricated. The joint dimensions were adapted from the ASTM D1002 standard, which serves as a guideline for testing the strength of adhesives in metal bonding. This standard is commonly employed for assessing the joining strength of polymer-metal hybrids.

Ti6Al4V substrates were cut and machined from rolled sheets into the symmetrical side of a half-lap splice joint (Figure 2). The recessed surface was structured using a pulsed laser to enhance adhesion with the polymer. A Trotec Speed Marker 50 instrument was used, featuring an average power of 20 watts, a wavelength of 1064 nm, a spot diameter of 40 µm, and a pulse duration of 110 ns. The frequency was set at 20 kHz and the scan speed at 500 mm/s. The laser beam

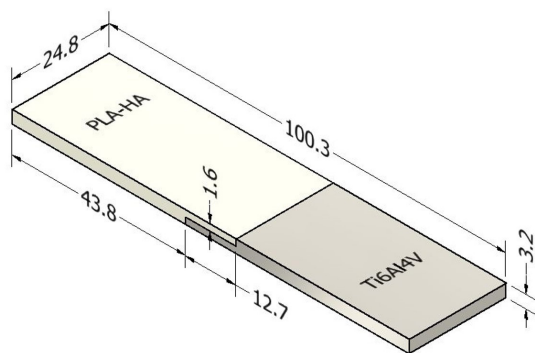


Figure 2. Schematic illustration of half-lap splice PLA–HA/Ti6Al4V hybrid joint specimens manufactured by injection overmolding. The dimensions are given in mm.

was scanned line by line in both directions with a line spacing of 100 µm. The laser was first scanned in one direction back and forth until the entire area of the metal insert recess was covered. The scanning was then repeated in the orthogonal direction. The procedure was carried out a total of four times. Before each step of surface structuring and injection molding, the metal parts were rinsed with compressed air followed by immersion in isopropyl alcohol in an ultrasonic bath for 3 min. The surface of the laser-structured Ti6Al4V part was analyzed using scanning electron microscopy (SEM) with an FEI Inspect S50 instrument at an acceleration voltage of 25 kV. Additionally, laser confocal microscopy was performed using an Olympus LEXT OLS4100 instrument with a wavelength of 405 nm.

The hybrid joints were fabricated using an Arburg Allrounder 270V 300-120 injection molding machine. The machine was operated in semi-automatic mode, where the metal substrate was manually placed in the mold cavity before initiating the injection molding cycle. The optimized operating conditions included a barrel temperature of 200°C, an injection speed of 30 cm³/s, a holding pressure of 500 bar, a holding time of 7 seconds, a mold temperature of 25°C, and a cooling time of 30 seconds.

Lap-shear testing was conducted according to a modified version of the ASTM D1002 standard, using an Instron 5569 system. The distance between grips was set to 60 mm, and the test was conducted at a crosshead speed of 1.27 mm/min. Five replicate specimens were tested, which were conditioned at 23°C and 50% relative humidity for 48 hours before testing.

The cross-section of the hybrid joint was analyzed using optical microscopy with a LEXT OLS 4100 (Olympus, Japan) instrument. The specimen was sectioned, embedded in epoxy resin, and polished prior to examination.

3. Results and Discussion

3.1 PLA–HA biocomposite

The morphology of hydroxyapatite (HA) and its dispersion within the PLA–HA biocomposite were evaluated using SEM, with representative images displayed in Figure 3a-b. HA appears as compact agglomerates of globular particles with size in

the range of 150 to 250 nm (Figure 3a), which are typical of the synthesis route adopted^[20]. In the biocomposite, HA is in the form of small clusters of approximately 2-5 particles (< 1 μm) well distributed in the PLA matrix (Figure 3b). This indicates that the melt-processing route adopted was efficient in dispersing and distributing the HA in the polymer matrix. The dispersion of sub-micrometer-sized particles, especially those capable of forming hydrogen bonds like the HA used in this study, is hindered by their high surface energy, which can lead to agglomeration^[9,10]. On the other hand, PLA is polar and has the ability to form hydrogen bonds with HA. These interactions create a robust polymer/particle interface, which facilitates the dispersion and distribution of particles within the polymer matrix during the melting process^[7]. Moreover, the mixing energy generated by the applied shear stress during the melt-compounding of the PLA-HA biocomposite can surpass the cohesive energy between the HA particles^[22]. The literature indicates that the dispersion of HA particles on a submicron scale offers

a high surface area to volume ratio, which increases the mechanical properties and bioactivity of the material^[4].

The thermal decomposition behavior of the PLA matrix in the PLA-HA biocomposite was evaluated by thermogravimetric analysis (TGA). The TG and derivative (DTG) curves for neat PLA (control), PLA-HA biocomposite and neat hydroxyapatite HA (control) are shown in Figure 4. Thermal decomposition data are shown in Table 1. HA exhibits thermal stability, showing no measurable weight loss up to 800°C. Both PLA and PLA-HA biocomposite exhibited a single-step thermal decomposition event. This behavior has been attributed to the depolymerization of PLA, resulting in the formation of oligomers and lactides^[23,24]. The residual mass of PLA consists of char, whereas for the PLA-HA biocomposite, it additionally consists of undecomposed hydroxyapatite (HA). The PLA-HA biocomposite exhibited slightly lower decomposition temperatures compared to neat PLA, which may be attributed to the prior degradation that PLA experienced during the melt processing of the PLA-HA

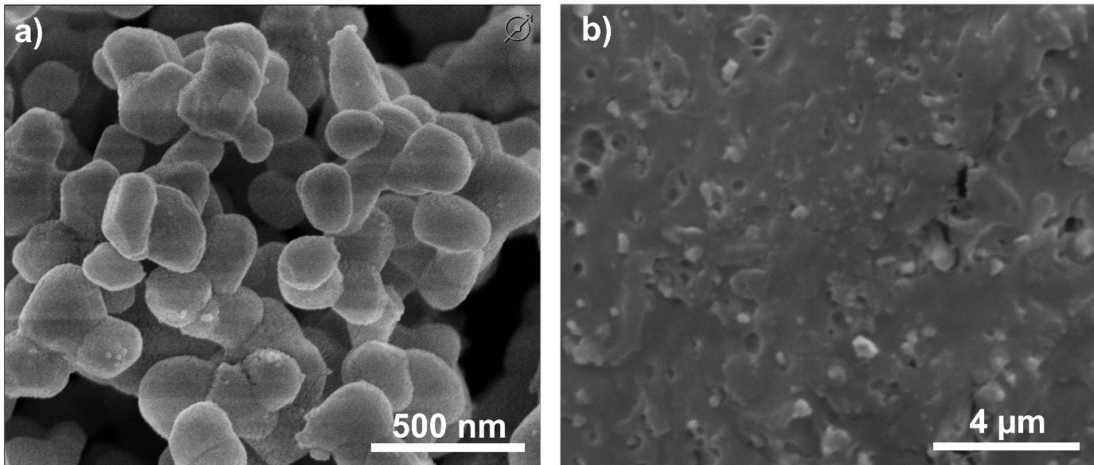


Figure 3. Scanning electron microscopy (SEM) images of the hydroxyapatite (HA) (a) and PLA-HA biocomposite (b).

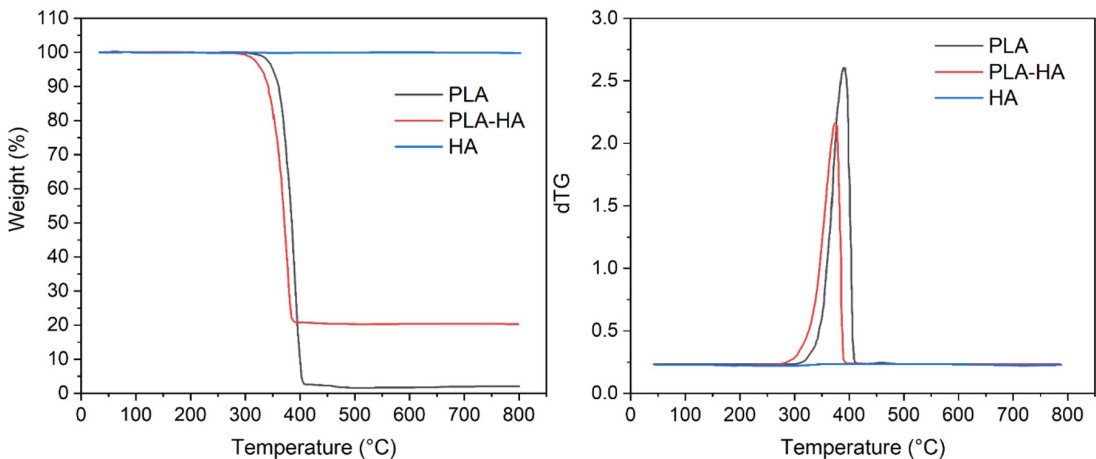


Figure 4. Thermogravimetric (TG) and derivative thermogravimetric (dTG) curves for neat PLA, PLA-HA biocomposite and neat HA under N_2 atmosphere.

biocomposite. Dedicated studies reported in the literature have shown that melt processing can induce thermomechanical degradation of PLA through chain scission, leading to a decrease in molecular weight^[25,26].

The crystallinity behavior of the PLA matrix in both neat PLA (control) and PLA–HA biocomposite injection-molded parts was evaluated using MDSC analysis. The MDSC curves are shown in Figure 5, and the data are summarized in Table 2. MDSC is a more reliable technique than standard DSC for measuring the crystallinity behavior of polymers with low crystallization kinetics, such as PLA. The cold crystallization of PLA appears as an exothermic peak in the non-reversing curve. The maximum cold crystallization temperature of PLA in the PLA–HA biocomposite shifts to a lower temperature by approximately 5 °C, indicating that hydroxyapatite acts as a heterogeneous nucleating agent for the PLA matrix. Additionally, the degradation of PLA during compounding with HA, as indicated by the TGA analysis (Figure 4; Table 1), may also have contributed to the reduction in the cold crystallization temperature. The cold crystallization enthalpy of PLA, measured from the non-reversing signal and normalized to the PLA content in the sample, is nearly equivalent between the PLA–HA biocomposite and neat

PLA. Melting occurs over a wide range of temperatures, beginning shortly after cold crystallization, as indicated by the endothermic peak observed in the non-reversing signal. This melting is accompanied by recrystallization, observed as an exothermic event in the reversing signal. This process is associated with crystal perfection, where smaller and less perfect crystals melt and recrystallize successively, using the remaining crystals as templates to form more perfect structures. The enthalpies related to crystal perfection, normalized to the PLA content in the sample, are higher in the neat PLA sample compared to the PLA–HA biocomposite. This indicates that the previous thermal history (injection molding) of the PLA in the PLA–HA biocomposite resulted in more perfect crystals, making them less susceptible to the crystal perfection phenomenon.

The degrees of crystallinity of PLA in both the neat PLA and PLA–HA biocomposite samples, related to their previous crystallization history (injection molding) and independent of the thermal history acquired during DSC heating, were calculated using Equation 1. The terms in Equation 1 are defined as follows: $\Delta H_m^{non-reversing}$ is the melting enthalpy measured in the non-reversing curve; $\Delta H_{cc}^{non-reversing}$ is the cold crystallization enthalpy measured in the non-reversing

Table 1. Thermogravimetric data for neat PLA (control) and PLA–HA biocomposite under N₂ atmosphere.

Sample	T _{start} (°C)	T _{peak} (°C)	T _{end} (°C)	Mass residue (%)
PLA	303	388	413	1.9
PLA–HA	275	375	394	20.1

Table 2. MDSC data for neat PLA (control) and PLA–HA biocomposite. The data are normalized to the PLA content in each sample.

Sample	$\Delta H_{cc}^{non-reversing}$	$\Delta H_m^{non-reversing}$	$\Delta H_{rec}^{reversing}$	X_c
	(J g ⁻¹)	(J g ⁻¹)	(J g ⁻¹)	
PLA	25.2	49.3	20.2	4
PLA–HA	22.8	36.8	4.4	10

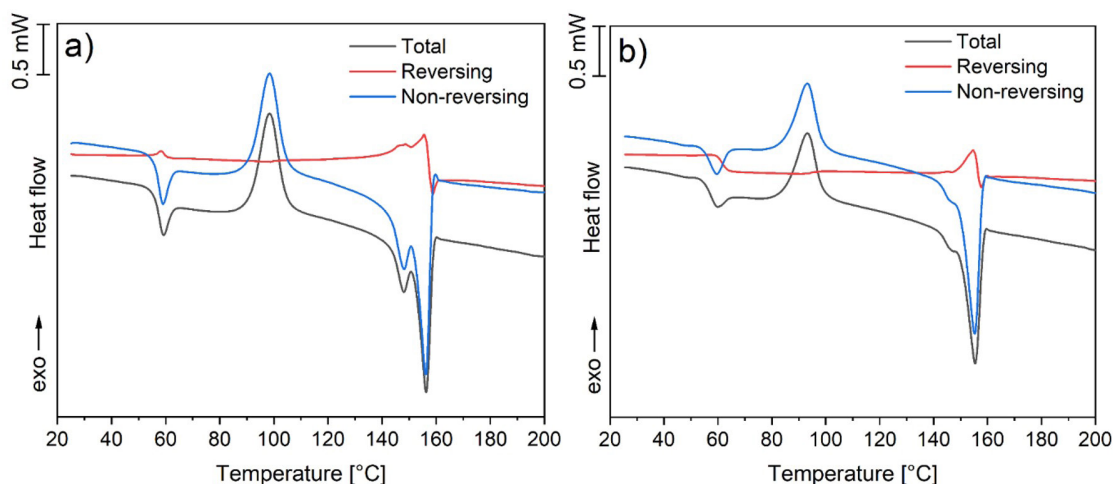


Figure 5. MDSC curves for neat PLA (control) (a) and PLA–HA biocomposite (b).

curve; $\Delta H_{rec}^{reversing}$ is the recrystallization enthalpy related to crystal perfection phenomena measured in the reversing curve; and $\Delta H_m^{100\%}$ is the melting enthalpy for 100% crystalline PLA (93 J/g^[6]). All enthalpies are normalized to the PLA content in each sample.

$$X_c = \frac{\Delta H_m^{non-reversing} - \Delta H_{cc}^{non-reversing} - \Delta H_{rec}^{reversing}}{\Delta H_m^{100\%}} \quad (1)$$

Therefore, the MDSC analysis demonstrated that PLA crystallization is enhanced in the presence of HA, leading to greater crystal perfection and a higher degree of crystallinity in injection-molded samples. This finding corroborates the results of other studies on PLA–HA composites^[5-7].

The mechanical behavior of the PLA–HA biocomposite was evaluated through tensile and flexural tests. PLA specimens were tested for comparison. Mechanical properties are shown in Table 3.

In tensile tests, PLA exhibited ductile behavior, though fracture occurred shortly after yielding. In contrast, the PLA–HA biocomposite displayed brittle behavior, with fracture occurring at a slightly lower stress level than that for the yielding of the neat PLA. The increase in modulus with HA incorporation into PLA is achieved at the expense of tensile strength and strain at break. A similar trend was observed in the flexural test, where the incorporation of HA into PLA resulted in an increased modulus but a decrease in flexural strength. In general, the mechanical behavior observed in this study for the PLA–HA biocomposite is similar to that reported in the literature for other biocomposites processed in the molten state with similar filler contents^[6,7]. The increased stiffness of PLA upon incorporating HA particles are attributed in the literature to the mechanical

anchoring of PLA chains around the HA particles, which restricts the movement of PLA chains and hinders the deformation of the PLA matrix^[6,7]. The modest increase in modulus, along with the lower mechanical strength and elongation at break, can be attributed to the low aspect ratio of the nearly spherical HA particles (Figure 3a), despite their fine dispersion and good distribution within the PLA matrix (Figure 3b). The increased degree of crystallinity in the PLA matrix (Table 2) may have also contributed to the enhanced modulus, while decreasing the strength and elongation at break of the biocomposite. On the other hand, the degradation of PLA during compounding with HA, as indicated by the TGA analysis (Figure 4; Table 1), may have negatively affected the modulus, strength, and elongation at break.

3.2 PLA–HA/Ti6Al4V hybrid joint

The topography of the laser-surface-structured Ti6Al4V substrate was analyzed using scanning electron microscopy (SEM) and confocal laser microscopy, and the images are shown in Figure 6a-b. Laser structuring produced structures in the form of valleys and hills arranged in a square grid of 100 × 100 μm. The valleys are formed by the material removed by laser ablation, while the hills are formed by the re-solidified metal, often referred to as remelted metal, which is expelled and deposited in the space between the valleys. The average width and depth of the valleys were 57 ± 5 μm and 55 ± 9 μm, respectively, and the average width and height of the hills were 50 ± 7 μm and 27 ± 7 μm, respectively.

Figure 7 shows the lap-shear force-displacement curves for the PLA–HA/Ti6Al4V hybrid joint specimens. Similar patterns were observed among the examined specimens, indicating the robust repeatability of the adopted laser structuring and injection overmolding methodology.

Table 3. Mechanical properties of PLA (control) and PLA–HA biocomposite in tensile and flexural tests.

Material	Tensile Modulus (GPa)	Tensile Strength (GPa)	Strain at Break (%)	Flexural Modulus (GPa)	Flexural Strength (GPa)
PLA (control)	4.8 ± 0.6	63.9 ± 1.1*	3.1 ± 0.2	3.6 ± 0.3	104.4 ± 1.8
PLA–HA biocomposite	5.4 ± 0.3	59.9 ± 0.7**	1.9 ± 0.1	4.7 ± 0.1	93.3 ± 3.7

*Tensile stress at yield. **Tensile stress at break.

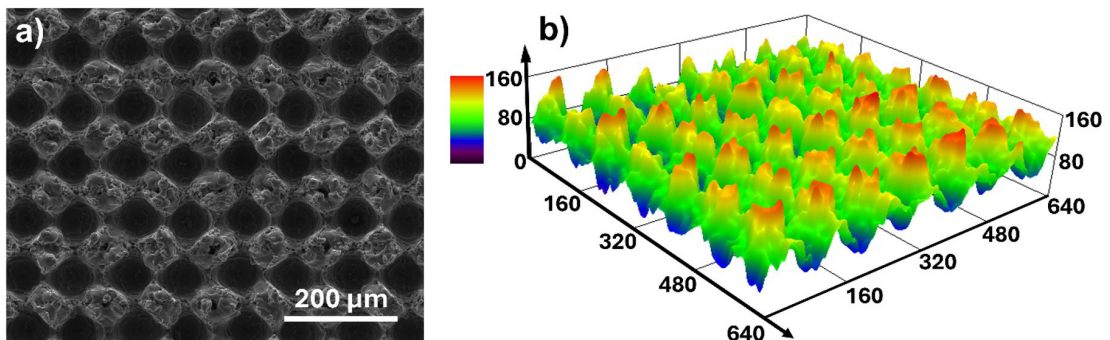


Figure 6. Scanning electron microscopy (SEM) (a) and confocal laser microscopy (b) images of the surface of laser-structured Ti6Al4V substrate.

All specimens exhibited macroscopic failure due to brittle fracture of the PLA–HA part outside the bonding zone, near the end of the metal part, as shown in Figure 8. The PLA–HA/Ti6Al4V joint exhibited an ultimate lap-shear force (ULSF) of 1190 ± 21 N and displacement at break of 0.33 ± 0.03 mm. The mechanical performance of the PLA–HA/Ti6Al4V joints was slightly lower than that of the joints fabricated with neat PLA, which exhibited an ULSF of 1592 ± 28 N and a displacement at break of 0.84 ± 0.23 mm. This trend is consistent with the behavior observed in the tensile tests (Table 3). The ULSF of the PLA–HA/Ti6Al4V joint is approximately 50% of the nominal force required for the PLA–HA part to break, based on its tensile strength of 59.9 ± 0.7 MPa (Table 3). This behavior is to be expected in an overlap hybrid joint specimen with a polymeric component exhibiting brittle mechanical behavior, such as PLA–HA. In the lap-shear test of half-lap splice joints, such as that employed in this study, the polymeric component is subjected to complex strain fields involving tension, shear, and bending, resulting in fracture occurring at lower stress levels than those observed in a tensile test^[27]. In contrast, overlap hybrid joints with polymer components exhibiting ductile behavior can withstand stresses in the lap-shear test

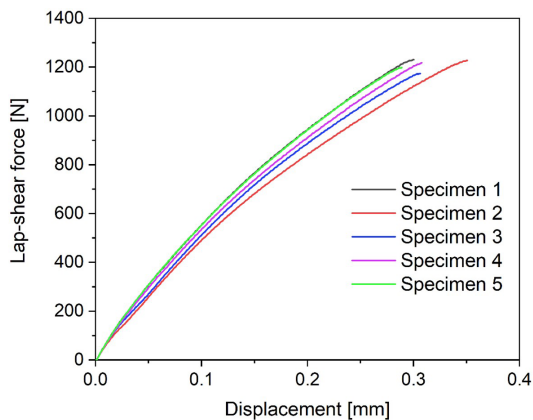


Figure 7. Lap-shear curves for PLA–HA/Ti6Al4V hybrid joint specimens. Each of the five replicate specimens is given a corresponding number in the figure legend.

that are very close to those obtained in the tensile test for the polymer component^[17,18].

The good mechanical anchorage at the interface between the PLA–HA biocomposite and the structured surface of the Ti6Al4V substrate was due to the complete filling of the metal cavities with the biocomposite, as shown in the cross-section view of the PLA–HA/Ti6Al4V hybrid joint (Figure 9). In injection overmolding, the degree to which a polymer fills micro-patterns on a metal surface is contingent upon the process parameters. In general, any parameter that reduces the thickness of the frozen polymer layer and compensates for shrinkage during solidification has a positive effect^[15,19]. Therefore, in the injection overmolding process of the PLA–HA/Ti6Al4V joint specimens, the barrel and mold temperatures, along with the injection speed, holding pressure, and holding time, were optimized within the PLA processing window to ensure full penetration of the polymer biocomposite into the micro-scale features on the metal surface. It is suggested that mechanical interlocking is the main adhesion mechanism for the PLA–HA/Ti6Al4V joint. Nevertheless, there is speculation that adsorption and chemical bonding may serve as possible secondary mechanisms. Interfacial adhesion is primarily influenced by the interaction between the PLA surface layer of the biocomposite part and the oxide layer of the metal surface. Hydroxyapatite (HA) particles in the PLA–HA composite are not expected to directly affect the adhesion with the Ti6Al4V substrate. This is because, in the injection molding of polymer composites, a thin, filler-free polymer skin is formed on the surface of the composite part. This prevents contact between the HA particles of the biocomposite and the metal surface during injection overmolding of PLA–HA/Ti6Al4V hybrid joint. Chemical interactions at the joint interface may occur between the ester groups of the PLA chains and the oxide layer on the metal surface. This hypothesis is based on a study that, through X-ray photoelectron spectroscopy (XPS) measurements and a critical review of the literature, suggested the formation of covalent bonds between polymers containing carbonyl groups and the oxide layer of metal substrates^[28].

The good mechanical performance of the injection overmolded PLA–HA/Ti6Al4V joints indicates they are promising for the development of hybrid structures for biomedical applications, especially in the field of orthopedics.

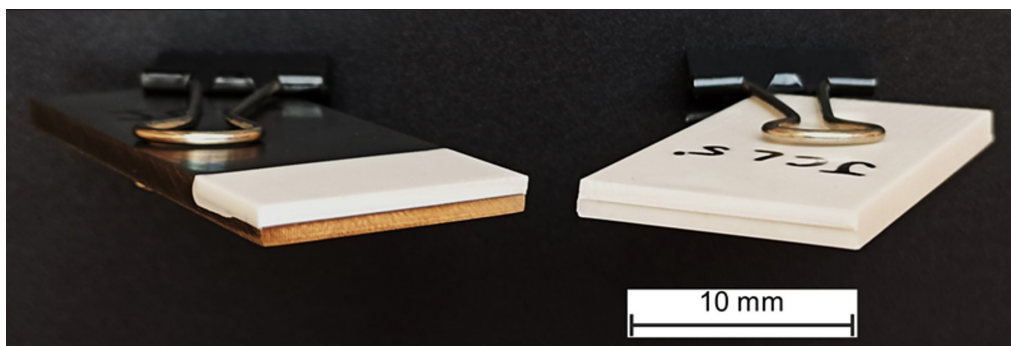


Figure 8. Image of an PLA–HA/Ti6Al4V hybrid joint specimen subjected to lap-shear testing, showing the transverse brittle fracture of PLA–HA biocomposite outside the bonding zone, near the end of the metal part.

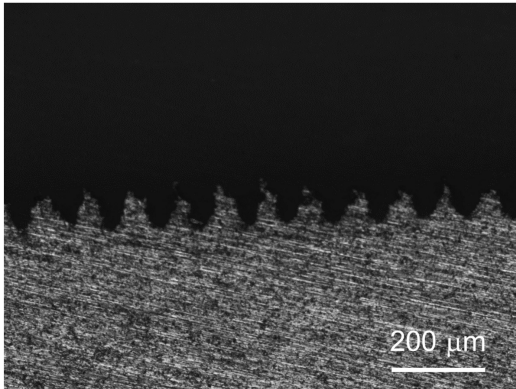


Figure 9. Cross-section optical microscopy image of the PLA–HA/Ti6Al4V hybrid joint. Polymer is on the top, and metal is on the bottom.

However, in practical applications, the mechanical performance of this joint warrants further assessment with regard to additional criteria, including temperature and media exposure simulating biological systems.

4. Conclusions

A methodology has been devised for fabricating a robust hybrid overlap structure consisting of a polylactide acid–hydroxyapatite (PLA–HA) biocomposite with titanium alloy Ti6Al4V. The procedure consisted of developing the PLA biocomposite with 20 wt% of nearly spherical sub-micron HA particles by melt processing, laser surface structuring of the Ti6Al4V, followed by injection overmolding of the PLA–HA biocomposite onto the surface-structured Ti6Al4V. This ensured effective anchoring of the polymer biocomposite to the metal part, leading to high shear strength in the joints, with the fracture of the polymer component occurring outside the bonding zone. The promising mechanical performance exhibited by the injection overmolded PLA–HA/Ti6Al4V joint suggests their potential for advancing hybrid structures in biomedical applications, particularly within the orthopedic field.

5. Author's Contribution

- **Conceptualization** – Márcio Antônio Fiori; Leonardo Bresciani Canto.
- **Data curation** – Renan Adauto; Gean Henrique Marcatto de Oliveira; Mário Augusto Morozo.
- **Formal analysis** – Renan Adauto; Gean Henrique Marcatto de Oliveira; Mário Augusto Morozo.
- **Funding acquisition** – Márcio Antônio Fiori; Leonardo Bresciani Canto.
- **Investigation** – Renan Adauto; Gean Henrique Marcatto de Oliveira; Mário Augusto Morozo.
- **Methodology** – Márcio Antônio Fiori; Leonardo Bresciani Canto.
- **Project administration** – Márcio Antônio Fiori; Leonardo Bresciani Canto.

- **Resources** – Márcio Antônio Fiori; Leonardo Bresciani Canto.
- **Software** – NA.
- **Supervision** – Márcio Antônio Fiori; Leonardo Bresciani Canto.
- **Validation** – Márcio Antônio Fiori; Leonardo Bresciani Canto.
- **Visualization** – Renan Adauto; Gean Henrique Marcatto de Oliveira; Leonardo Bresciani Canto.
- **Writing – original draft** – Renan Adauto; Gean Henrique Marcatto de Oliveira; Leonardo Bresciani Canto.
- **Writing – review & editing** – Renan Adauto; Gean Henrique Marcatto de Oliveira; Leonardo Bresciani Canto.

6. Acknowledgements

This study was supported by FAPESP – São Paulo Research Foundation, Brazil (grant number 2018/24296-0), CNPq – National Council for Scientific and Technological Development, Brazil (grant numbers 309258/2020-0, 132355/2020-5 and 164791/2018-3) and CAPES – Coordenação de Aperfeiçoamento de Pessoal de Nível Superior – Brazil (grant number 23038.021524.2016.88). This study was financed in part by the Coordenação de Aperfeiçoamento de Pessoal de Nível Superior - Brasil (CAPES) – Finance Code 001. The authors are grateful to the Laboratory of Structural Characterization (LCE/DEMA/UFSCar) for use of the general facilities.

7. References

1. Liu, S., Qin, S., He, M., Zhou, D., Qin, Q., & Wang, H. (2020). Current applications of poly(lactic acid) composites in tissue engineering and drug delivery. *Composites. Part B, Engineering*, 199, 108238. <http://doi.org/10.1016/j.compositesb.2020.108238>.
2. Pérez-Davila, S., Garrido-Gulías, N., González-Rodríguez, L., López-Álvarez, M., Serra, J., López-Periago, J. E., & González, P. (2023). Physicochemical properties of 3D-printed polylactic acid/hydroxyapatite scaffolds. *Polymers*, 15(13), 2849. <http://doi.org/10.3390/polym15132849>. PMID:37447495.
3. Wang, W., Zhang, B., Li, M., Li, J., Zhang, C., Han, Y., Wang, L., Wang, K., Zhou, C., Liu, L., Fan, Y., & Zhang, X. (2021). 3D printing of PLA/n-HA composite scaffolds with customized mechanical properties and biological functions for bone tissue engineering. *Composites. Part B, Engineering*, 224, 109192. <http://doi.org/10.1016/j.compositesb.2021.109192>.
4. Zhou, H., Lawrence, J. G., & Bhaduri, S. B. (2012). Fabrication aspects of PLA–CaP/PLGA–CaP composites for orthopedic applications: A review. *Acta Biomaterialia*, 8(6), 1999–2016. <http://doi.org/10.1016/j.actbio.2012.01.031>. PMID:22342596.
5. Senatov, F. S., Niaza, K. V., Zadorozhnyy, M. Y., Maksimkin, A. V., Kaloshkin, S. D., & Estrin, Y. Z. (2016). Mechanical properties and shape memory effect of 3D-printed PLA-based porous scaffolds. *Journal of the Mechanical Behavior of Biomedical Materials*, 57, 139–148. <http://doi.org/10.1016/j.jmbm.2015.11.036>. PMID:26710259.
6. Ferri, J. M., Jordá, J., Montanes, N., Fenollar, O., & Balart, R. (2018). Manufacturing and characterization of poly(lactic acid) composites with hydroxyapatite. *Journal of Thermoplastic Composite Materials*, 31(7), 865–881. <http://doi.org/10.1177/0892705717729014>.

7. Kryszak, B., Biernat, M., Tymowicz-Grzyb, P., Junka, A., Brozyna, M., Worek, M., Dzienny, P., Antonczak, A., & Szustakiewicz, K. (2023). The effect of extrusion and injection molding on physical, chemical, and biological properties of PLLA/HAp whiskers composites. *Polymer*, *287*, 126428. <http://doi.org/10.1016/j.polymer.2023.126428>.
8. Watai, J. S., Calvão, P. S., Rigolin, T. R., Bettini, S. H. P., & Souza, A. M. C. (2020). Retardation effect of nanohydroxyapatite on the hydrolytic degradation of poly (lactic acid). *Polymer Engineering and Science*, *60*(9), 2152-2162. <http://doi.org/10.1002/pen.25459>.
9. Abere, D. V., Ojo, S. A., Oyatogun, G. M., Paredes-Epinosa, M. B., Niluxsshun, M. C. D., & Hakami, A. (2022). Mechanical and morphological characterization of nano-hydroxyapatite (nHA) for bone regeneration: a mini review. *Biomedical Engineering Advances*, *4*, 100056. <http://doi.org/10.1016/j.bea.2022.100056>.
10. Lim, Q. R. T., Cheng, X. Y., & Wee, C. Y. (2023). An insight to the various applications of hydroxyapatite. *Advanced Materials Science and Technology*, *5*(2), 0520879. <http://doi.org/10.37155/2717-526X-0502-1>.
11. Koju, N., Niraula, S., & Fotovvati, B. (2022). Additively manufactured porous Ti6Al4V for bone implants: a review. *Metals*, *12*(4), 687. <http://doi.org/10.3390/met12040687>.
12. Sidambe, A. T. (2014). Biocompatibility of advanced manufactured titanium implants-a review. *Materials (Basel)*, *7*(12), 8168-8188. <http://doi.org/10.3390/ma7128168>. PMID:28788296.
13. Fereiduni, E., Mahmoud, D., Balbaa, M., & Elbestawi, M. (2022). Laser powder bed fusion of hydroxyapatite functionalized Ti-6Al-4V biomaterial with potential biomedical applications. *Materials Letters*, *326*, 132973. <http://doi.org/10.1016/j.matlet.2022.132973>.
14. Sukhodub, L. F., Sukhodub, L. B., Simka, W., & Kumeda, M. (2019). Hydroxyapatite and brushite coatings on plasma electrolytic oxidized Ti6Al4V alloys obtained by the thermal substrate deposition method. *Materials Letters*, *250*, 163-166. <http://doi.org/10.1016/j.matlet.2019.05.018>.
15. Vasconcelos, R. L., Oliveira, G. H. M., Amancio-Filho, S. T., & Canto, L. B. (2023). Injection overmolding of polymer-metal hybrid structures: a review. *Polymer Engineering and Science*, *63*(3), 691-722. <http://doi.org/10.1002/pen.26244>.
16. Grujicic, M., Sellappan, V., Omar, M. A., Seyr, N., Obieglo, A., Erdmann, M., & Holzleitner, J. (2008). An overview of the polymer-to-metal direct-adhesion hybrid technologies for loadbearing automotive components. *Journal of Materials Processing Technology*, *197*(1-3), 363-373. <http://doi.org/10.1016/j.jmatprotec.2007.06.058>.
17. Luiz, G. M., Oliveira, G. H. M., & Canto, L. B. (2024). Development of polyamide 6-graphene oxide nanocomposite and direct-joining with aluminum alloy for lightweight engineering applications. *Polymer Engineering and Science*, *64*(2), 663-674. <http://doi.org/10.1002/pen.26575>.
18. Oliveira, G. H. M., Morozo, M. A., Fiori, M. A., & Canto, L. B. (2024). A method for manufacturing a mechanically strong and durable hybrid structure of polyethylene-hydroxyapatite composite and titanium alloy. *Polymer Engineering and Science*, *64*(4), 1548-1554. <http://doi.org/10.1002/pen.26644>.
19. Oliveira, G. H. M., Amancio-Filho, S. T., & Canto, L. B. (2024). Processing understanding, mechanical durability and hygrothermal stability of PC/AA6061 hybrid joints produced via injection overmolding. *International Journal of Adhesion and Adhesives*, *130*, 103617. <http://doi.org/10.1016/j.ijadhadh.2023.103617>.
20. Morozo, M. A., Duarte, G. W., Silva, L. L., Mello, J. M. M., Zanetti, M., Colpani, G. L., Fiori, M. A., & Canto, L. B. (2023). A Design of Experiments Approach to analyze the effects of hydroxyapatite and maleic anhydride grafted polyethylene contents on mechanical, thermal and biocompatibility properties of green high-density polyethylene-based composites. *Materials Research*, *26*(suppl. 1), e20220548. <http://doi.org/10.1590/1980-5373-mr-2022-0548>.
21. Tanaka, F. H., Cruz, S. A., & Canto, L. B. (2018). Morphological, thermal and mechanical behavior of sepiolite-based poly(ethylene terephthalate)/polyamide 66 blend nanocomposites. *Polymer Testing*, *72*, 298-307. <http://doi.org/10.1016/j.polymertesting.2018.10.027>.
22. Sharifzadeh, E., & Maleki, M. (2022). An energy-based approach to study the aggregation/agglomeration phenomenon in polymer nanocomposites: dispersion force against inter-particle cohesion. *Polymer Composites*, *43*(8), 5145-5158. <http://doi.org/10.1002/pc.26804>.
23. Benhami, V. M. L., Longatti, S. M. O., Moreira, F. M. S., & Sena Neto, A. R. (2024). Biodegradation of poly(lactic acid) waste from 3D printing. *Polímeros: Ciência e Tecnologia*, *34*(2), e20240013. doi:10.1590/0104-1428.20230058
24. Fan, Y., Nishida, H., Shirai, Y., Tokiwa, Y., & Endo, T. (2004). Thermal degradation behaviour of poly(lactic acid) stereocomplex. *Polymer Degradation & Stability*, *86*(2), 197-208. <http://doi.org/10.1016/j.polymdegradstab.2004.03.001>.
25. Gonçalves, L. M. G., Rigolin, T. R., Frenhe, B. M., & Bettini, S. H. P. (2020). On the recycling of a biodegradable polymer: multiple extrusion of poly (lactic acid). *Materials Research*, *23*(5), e20200274. <http://doi.org/10.1590/1980-5373-mr-2020-0274>.
26. Backes, E. H., Pires, L. N., Costa, L. C., Passador, F. R., & Pessan, L. A. (2019). Analysis of the degradation during melt processing of PLA/Biosilicate® composites. *Journal of Composites Science*, *3*(2), 52. <http://doi.org/10.3390/jcs3020052>.
27. Oliveira, G. H. M., Sciuti, V. F., Canto, R. B., Armeitz, S., Minkowitz, L., Amancio-Filho, S. T., & Canto, L. B. (2024). Additive manufacturing of surface structured metal parts for high strength lightweight injection overmolded polymer-metal hybrid joints. *International Journal of Adhesion and Adhesives*.
28. Liu, F. C., Dong, P., Lu, W., & Sun, K. (2019). On formation of Al-O-C bonds at aluminum/polyamide joint interface. *Applied Surface Science*, *466*, 202-209. <http://doi.org/10.1016/j.apsusc.2018.10.024>.

Received: Sept. 25, 2024

Revised: Dec. 05, 2024

Accepted: Dec. 11, 2024